Force constant calibration corrections for silicon position detectors in the near-infrared

J. H. G. Huisstede, K. O. van der Werf, M. L. Bennink, and V. Subramaniam

Biophysical Engineering and MESA+ institute for nanotechnology, Department of Science and Technology, University of Twente, P.O. Box 217, 7500 AE Enschede, The Netherlands

v.subramaniam@utwente.nl

Abstract: The accurate calibration of the force constant of the probe in atomic force microscopy and optical tweezers applications is extremely important for force spectroscopy. The commonly used silicon detectors exhibit a complex transfer function for wavelengths >850 nm, which limits the detection bandwidth leading to serious errors in the force constant determination. We show that this low-pass effect can be compensated for using the frequency response of the detector. This is applicable for calibrations in both atomic force microscopy and optical tweezers. For optical tweezers an additional correction method is discussed based on fitting an expression in which the low-pass characteristics are already accounted for.

OCIS codes: (040.5160) Photodetectors; (040.6040) Silicon; (230.5160) Photodetectors; (230.0250) Optoelectronics

References and links

1. G. U. Lee, D. A. Kidwell and R. J. Colton, "Sensing discrete streptavidin biotin interactions with atomic-force microscopy," Langmuir **10** 354–357 (1994).
2. P. Hinterdorfer, W. Baumgartner, H. J. Gruber, K. Schilcher and H. Schindler, "Detection and localization of individual antibody-antigen recognition events by atomic force microscopy," PNAS **93,** 3477–3481 (1996).
3. M. Rief, M. Gautel, F. Oesterhelt, J. M. Fernandez and H. E. Gaub, "Reversible unfolding of individual titin immunoglobulin domains by afm," Science **276,** 1109–1112 (1997).
4. D. J. Muller, W. Baumeister and A. Engel, "Controlled unzipping of a bacterial surface layer with atomic force microscopy," PNAS **96,** 13170–13174 (1999).
5. F. Oesterhelt, D. Oesterhelt, M. Pfeiffer, A. Engel, H. E. Gaub and D. J. Muller, "Unfolding pathways of individual bacteriorhodopsins," Science **288** 143–146 (2000).
6. S. B. Smith, Y. J. Cui and C. Bustamante,"Overstretching b-dna: The elastic response of individual double-stranded and single-stranded dna molecules," Science **271,** 795–799 (1996).
7. M. S. Z. Kellermayer and C. Bustamante, "Folding-unfolding transitions in single titin molecules characterized with laser tweezers," Science **277,** 1117–1117 (1997).
8. D. E. Smith, S. J. Tans, S. B. Smith, S. Grimes, D. L. Anderson and C. Bustamante, "The bacteriophage phi 29 portal motor can package dna against a large internal force," Nature **413** 748–752 (2001).
9. M. L. Bennink, S. H. Leuba, G. H. Leno, J. Zlatanova, B. G. de Grooth and J. Greve, "Unfolding individual nucleosomes by stretching single chromatin fibers with optical tweezers," Nat. Struct. Biol. **8,** 606–610 (2001).
10. E. A. Abbondanzieri, W. J. Greenleaf, J. W. Shaevitz, R. Landick and S. M. Block, "Direct observation of base-pair stepping by rna polymerase," Nature **438,** 460–465 (2005).
11. F. Reif. *Fundamentals of statistical and thermal physics*. McGraw-Hill, New York, 1965.
12. K. Berg-Sorensen, L. Oddershede, E. L. Florin and H. Flyvbjerg, "Unintended filtering in a typical photodiode detection system for optical tweezers," J. Appl. Phys. **93,** 3167–3176 (2003).
13. E. J. G. Peterman, M. A. van Dijk, L. C. Kapitein and C. F. Schmidt, "Extending the bandwidth of optical-tweezers interferometry," Rev. Sci. Instrum. **74** 3246–3249 (2003).

#69453 - $15.00 USD Received 28 March 2006; revised 8 September 2006; accepted 8 September 2006

14. K. C. Neuman and S. M. Block, "Optical trapping," Rev. Sci. Instrum. **75,** 2787–2809 (2004).
15. J.H.G. Huisstede, B.D. van Rooijen, K.O. van der Werf, M.L. Bennink and V. Subramaniam, "Dependence of silicon position-detector bandwidth on wavelength, power, and bias," Opt. Lett. **31**, 610–612 (2006).
16. K.O. van der Werf, C.A.J. Putman, B.G. de Grooth, F.B. Segerink, E.H. Schipper, N.F. van Hulst and J. Greve, "Compact standalone atomic force microscope," Rev. Sci. Instrum. **64** 2892 (1993).
17. R. Kassies, K. O. van der Werf, A. Lenferink, C. N. Hunter, J. D. Olsen, V. Subramaniam and C. Otto, "Combined afm and confocal fluorescence microscope for applications in bio-nanotechnology," J. Microsc. **217,** 109–16 (2005).
18. K. Svoboda and S. M. Block, "Biological applications of optical forces," Ann. Rev. Biophys. Biomol. Struct. **23,** 247–285 (1994).
19. K. Berg-Sorensen and H. Flyvbjerg, "Power spectrum analysis for optical tweezers," Rev. Sci. Instrum. **75,** 594–612 (2004).
20. J. H. G. Huisstede, K. O. van der Werf, M. L. Bennink and V. Subramaniam, "Force detection in optical tweezers using backscattered light," Opt. Express **13,** 1113–1123 (2005).

1. Introduction

In addition to high resolution imaging applications the atomic force microscope (AFM) has proven its usefulness in force spectroscopy in the (sub)nN force range where the microscope is used to measure mechanical properties of biomolecules and polymers and the strength of inter- and intra-molecular bonds [1, 2, 3, 4, 5]. In the (sub)pN force range a widely used force spectroscopy microscope are the optical tweezers (OT) used for measuring the mechanical properties and unfolding pathways of single molecules and for determining the forces involved in molecular interactions [6, 7, 8, 9, 10].

The appropriate calibration of the force constant of the probe in these microscopes is important for force spectroscopy. The probe, a cantilever in AFM and a micron-sized bead in OT, is subjected to thermal collisions of the surrounding medium that can be considered as a 'white-noise' thermal force, resulting in the so-called Brownian motion of the probe. The power spectral density (S_x) of the deflection signal therefore reflects the frequency response of the probe. Based on the equipartition theorem $\frac{1}{2}k_{pr}\left\langle x^2\right\rangle = \frac{1}{2}k_bT$ [11], such that the force constant k_{pr} of the probe can be derived by integrating the power spectral density yielding $\left\langle x^2\right\rangle$, which is the variance of the probe position. T is the absolute temperature and k_b is Boltzmanns constant.

An important issue for both applications is that silicon-based position detectors, the type of detector that is often required, can behave as a low-pass filter at frequencies $>$5 kHz for near-infrared light ($>$800 nm). The magnitude of this effect is a function of wavelength, incident light power and the bias voltage [12, 13, 14, 15]. Due to the low-pass effect the integral of S_x (yielding $\left\langle x^2\right\rangle$) will be underestimated resulting in an overestimated force constant. The LED-wobbler developed recently allowed us to determine the frequency response of a position detector up to 600 kHz with high accuracy [15]. This frequency response was used to compensate S_x. For optical tweezers an additional correction method is discussed based on fitting an expression in which the low-pass characteristics are already accounted for.

2. Results

The frequency response of the Brownian motion of a cantilever (MSCT-AUHW, Cantilever B, Veeco, New York) was measured in air in a custom-built AFM [16] with a 785 nm laser diode. The same cantilever was transferred to a hybrid AFM-confocal optical microscope [17] that uses a 1050 nm laser diode to prevent induced photo bleaching during simultaneous fluorescence (at 800 nm) and topography measurements. Both setups include the same type of detector (UDT, Spot9-DMI). Calibration of the detector by determining the deflection sensitivity (nm/Volt)is carried out in a range of 10-100 Hz. The power spectral densities for AFM shown in this letter were corrected for the background noise that was determined by switching

#69453 - $15.00 USD Received 28 March 2006; revised 8 September 2006; accepted 8 September 2006

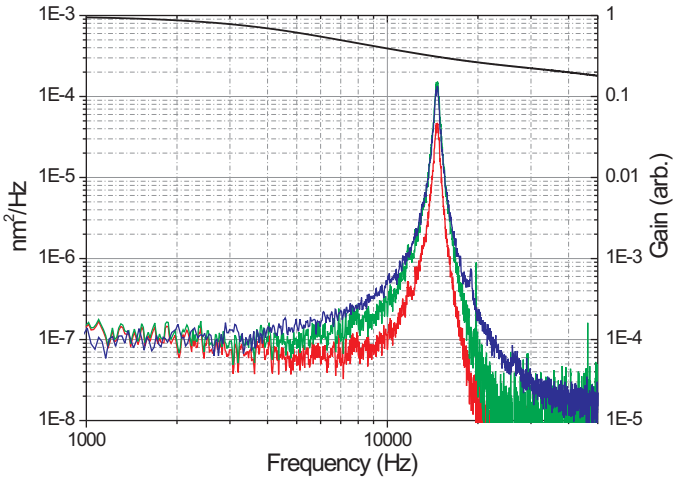

Fig. 1. Power spectral densities of a cantilever measured in an AFM with a laserdiode operating at 785 nm (blue curve) and a hybrid AFM/optical microscope with a laserdiode operating at 1050 nm (red curve). For the latter application a version of the curve corrected for the low-pass effect of the detector is shown (green curve). The gain of the detector used for correction is depicted by the black curve.

off the laser diode.

In Fig. 1 we show the power spectral density function (S_x) for the same cantilever as acquired in both setups (blue and red curve). The S_x at 1050 nm corrected for the frequency response of the detector is also given (green curve). The detector response (gain versus frequency) obtained with the LED-wobbler is depicted by the black curve.

According to the equipartition theorem [11] each mode of vibration of the cantilever equals an energy $\frac{1}{2}k_bT$ and therefore the first mode of vibration equals $\frac{1}{2}k_{pr}\langle x^2\rangle$. For a high Q-factor $\langle x^2\rangle$ can be approximated by integrating around the first resonance peak. Integrating the spectra (Fig. 1) from 6-21 kHz we found a stiffness of $(3.8\pm0.2)\cdot10^{-2}$ N/m for the probe acquired at a wavelength of 785 nm. At a wavelength of 1050 nm the calculated stiffness was $(11.1\pm0.6)\cdot10^{-2}$ N/m. That means that due to the low-pass effect the stiffness is overestimated by a factor of 3. After correcting S_x for the response of the detector the stiffness was found to be $(3.5\pm0.2)\cdot10^{-2}$ N/m, within 10% of the value at 785 nm.

In contrast to AFM, in OT applications the power spectral density S_x looks different (see Fig. 2, black circles) due to the fact that in this case the damping forces are dominant. The same method of integrating S_x can be applied, but in this case it is also possible to fit the spectrum with a Lorentzian function. From the cut-off frequency found here the trap stiffness can be deduced, even when the detector is not calibrated. The Lorentzian is given by

$$S_x = \frac{D/\pi^2}{f^2 + f_c^2} \tag{1}$$

where D is the diffusion constant, f the frequency and f_c the cut-off frequency. The trap stiffness is calculated according to $k_{tr} = 2\pi\gamma_0 f_c$ with γ_0 Stokes friction coefficient for a sphere [18]. In the Lorentzian curve-fitting procedure hydrodynamic and aliasing corrections were included [19].

We used three different position detectors to acquire spectra for a trapped 2.67 μm polystyrene bead in an optical tweezers setup (Bangs Labs, Fishers, IN) with a 2.5 W Nd:YAG

#69453 - $15.00 USD Received 28 March 2006; revised 8 September 2006; accepted 8 September 2006

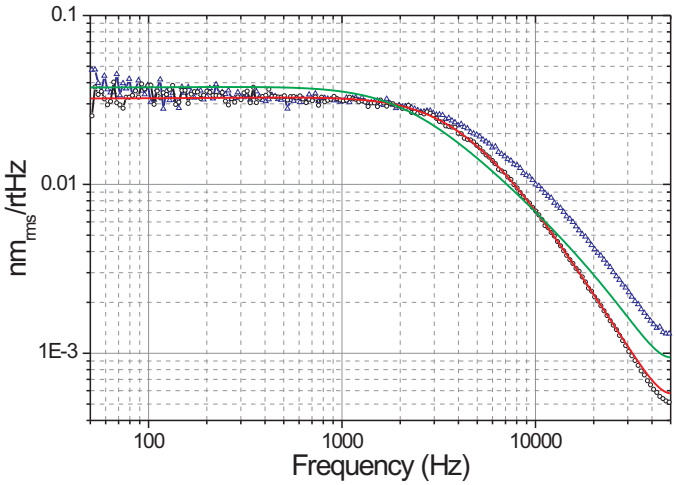

Fig. 2. Power spectral density of the deflection signal of a 2.67 μm polystyrene bead in an optical trap recorded with the SPOT9DMI (black circles). The spectrum corrected for the detector response is also plotted (blue triangulars). Furthermore the Lorentzian fit to the spectrum recorded with the SPOT9DMI including the model described by Eq. 2 (red curve) and without the model (green curve) is shown.

Table 1. Optical trap stiffness values determined by curve-fitting the power spectral density with a Lorentzian function. The power spectra for all detectors are obtained for the same 2.67 μm polystyrene bead. Two corrections methods for the low-pass effect of a silicon detector were investigated and compared with the situation where no corrections are applied.

Detector	Lorentzian, no corrections k_{trap} $(pN/\mu m)$	Lorentzian with corrected spectra k_{trap} $(pN/\mu m)$	Lorentzian with model lowpass effect f_{diode} (kHz)	α	k_{trap} $(pN/\mu m)$
DL100-7-KER 500μW	566	577	47.1 [1]		593
DL100-7-KER 150μW	566	575	17.3	0.83	599
DLS10 500μW	419	595	12.8	0.45	572
DLS10 150μW	401	595	10	0.48	590
SPOT9DMI 500μW	337	591	8.1	0.40	569
SPOT9DMI 150μW	323	574	6.7	0.38	599

laser (Coherent, Compass 1064-2500MN, Santa Clara, CA) operating at a wavelength of 1064 nm [9]. In contrast to AFM, the light power on the detector in OT applications can differ for various trapped beads and therefore the low-pass effect. In transmission-based OT the variation in intensity is approximately 10-20% and for a reflection-based setup it can be a factor of 2 [20]. To investigate the effect of light power, spectra were recorded at powers of 500 and 150 μW. Reduction of the light power was achieved by the use of a neutral density filter in front of the detector through which the optical trap was unaffected. The detectors used were the DL100-7-KER (Pacific Silicon Sensor), the DLS10 (UDT) and the SPOT-9DMI (UDT). Fig. 2 shows the power spectral density of a trapped bead acquired with the SPOT9-DMI (black circles).

First we demonstrate the influence of applying no corrections by fitting directly the Lorentzian function, given by Eq. 1 to the acquired spectra. The resulting Lorentzian fit is

#69453 - $15.00 USD Received 28 March 2006; revised 8 September 2006; accepted 8 September 2006

shown in Fig. 2 (green curve). The fit results for the uncorrected S_x for all three detectors at the two light powers are given in the second column of Table 1. If a detector that reveals a low-pass effect starting at lower frequencies was used, a lower value for the trap stiffness was found.

As for AFM applications S_x can be corrected for the frequency response of the detector as measured with the LED wobbler (at 1070 nm and the same light powers). After correction S_x is curve-fitted again with the Lorentzian function (Eq. 1). For all spectra the fit-range was 110 Hz - 10 kHz. The resulting optical trap stiffness values are given in the third column of Table 1 showing that the trap stiffness values deduced with the detectors are in good agreement with a variation of $<2\%$.

For OT a second method is available based on fitting an expression included in the Lorentzian function to account for the low-pass effect. Actually this expression for the low-pass effect, given by Eq. 2, is derived by Berg-Sørensen *et al.* (2003) to account for the low-pass effect and to circumvent the requirement to determine the total light power. Before discussing this correction method we validate the expression by fitting it to the frequency response of the detector as measured with the LED wobbler. The expression is given by

$$P_{diode} = \alpha^2 + \frac{1-\alpha^2}{1+(f/f_{diode})^2} \tag{2}$$

In this equation α describes the fraction of light absorbed in the depletion layer, which is a function of the effective thickness of the depletion layer and therefore a function of wavelength, bias voltage and light power. Since the fraction of light absorbed outside the depletion layer has to diffuse towards the depletion layer it is low-pass filtered with a characteristic frequency f_{diode}. Depending on the detector f_{diode} is in the order of 5 kHz. In Fig. 3 we show frequency responses of the DL100-7-KER, the DLS10 and the SPOT-9DMI for light powers of 50 and 500 μW. Additionally the fit based on Eq. 2 for each frequency response is shown. The model describes the effect quite well for lower frequencies. Above a certain frequency the model deviates significantly from the measured frequency response. The fit range was increased stepwise until the model did differ more than 5% from the value at the maximum frequency of the selected range (45 kHz for the DL100-7-KER, 15 kHz for the DLS10 and 10 kHz for the SPOT9DMI). For earlier results reported in the literature [12, 14] the frequency range was below these critical frequencies; consequently, this effect has not been observed before. For frequencies much higher than the characteristic frequency f_{diode} the second term in Eq. 2 approaches zero and the term, α^2 becomes dominant. Thus Eq. 2 will always be able to fit a low-pass filtered system up to a certain frequency, as long as the slope of the attenuation part is $\leq$6 dB/octave.

Now we use the Lorentzian function with the expression for the low-pass effect included, to fit to the power spectral densities for the 2.67 μm trapped bead trapped in the OT setup discussed previously. For this 'new' Lorentzian there are four fit parameters, D and f_c describing the dynamics of the trapped bead and α and f_{diode} describing the detector response. Again hydrodynamic and aliasing corrections are included. For all spectra the fit range was 110 Hz - 10 kHz. In Fig. 2 (red curve) the result is shown for this correction method. The resulting key fit parameters values are given in the last column of Table. 1. The trap stiffness values found for each detector are in good agreement. The trap stiffness found for the DL100-7-KER in the case no correction method was used is remarkably close to ($<5\%$) the values found for the two corrections methods, indicating the small low-pass effect of this detector. For the other two detectors the trap stiffness is strongly underestimated in case of no corrections. In separate experiments the trap stiffness values found with the two correction methods were compared with another calibration technique for OT (sinusoidal driving force [18]) where the trap stiffness did not differ more than $<5\%$ from this value.

#69453 - $15.00 USD Received 28 March 2006; revised 8 September 2006; accepted 8 September 2006

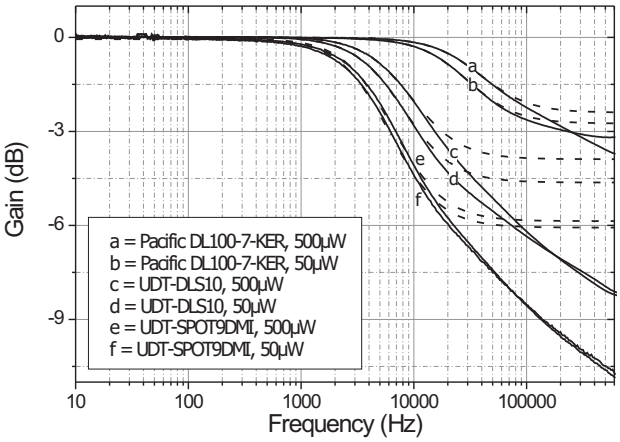

Fig. 3. Frequency response of the DL100-7-KER, the DLS10 and the SPOT9DMI determined with the LED-wobbler at 500 and 50 μW at 1070 nm. The dashed lines are the corresponding fits using Eq. 2. For the DLS10 the fit range was limited to 15 kHz, for the SPOT9-DMI to 10 kHz and for the DL100-7-KER to 45 kHz.

Finally we investigated the overall effect of the light power on the deduced trap stiffness using the first correction method discussed for both AFM and OT. Instead of correcting the spectra acquired at 500 μW with the frequency response of the detector at the appropriate power we used the detector response determined at 50 μW. For the DL100-7-KER we found a stiffness of 590 $pN/\mu m$ instead of 577 $pN/\mu m$ using the appropriate correction light power. For the DLS10 we found 654 $pN/\mu m$ instead of 595 $pN/\mu m$ and for the SPOT-9DMI 584 $pN/\mu m$ instead of 591 $pN/\mu m$. Although the difference in the power for the correction curves was a factor of 10, we found for both the DL100-7-KER and the SPOT9DMI an acceptable change of $< 3\%$. For the DLS10 a change of 10% was found.

3. Conclusion

Due to the low-pass effect of silicon position detectors large errors are found in the force constant determination in AFM and OT applications. However we have shown that the power spectral density can be corrected for the frequency response of the position detector as determined with the LED wobbler. Applying the equipartition theorem for AFM or curve-fitting a Lorentzian in OT the correct force constant can be determined. For variations of the light power within a factor of ten we found a variation of $<3\%$ for the force constant for the DL100-7-KER and the SPOT9-DMI. This makes acquisition of the frequency response of these two detectors for various powers redundant.

For OT an additional correction method is available by including a model for the detector low-pass effect into the Lorentzian curve-fit. However we have shown that this model partially describes the low-pass effect of the detector and is thus only applicable up to a maximum frequency range ($\sim$15 kHz). Knowledge of the frequency response of the detector beforehand is thus required.

Acknowledgements

This work is supported by the MESA+ institute for nanotechnology.

#69453 - $15.00 USD Received 28 March 2006; revised 8 September 2006; accepted 8 September 2006